Supplementary Information on 'The hydration structure of Cu^{2+}: More tetrahedral than octahedral?'

Daniel T. Bowron,[a] Monica Amboage,[b] Roberto Boada,[b,c,d] Adam Freeman,[b] Shu Hayama,[b] and Sofia Díaz-Moreno,[b]

[a] *ISIS Facility, Rutherford Appleton Laboratory, Chilton, Didcot, OX11 0QX, United Kingdom. Fax: +44 (0)1235 445720; Tel: +44 (0)1235 446381; E-mail: daniel.bowron@stfc.ac.uk*
[b] *Diamond Light Source Ltd., Diamond House, Harwell Science and Innovation Campus, Didcot, Oxfordshire, OX11 0DE, United Kingdom.*
[c] *Instituto de Ciencia de Materiales de Aragón, Consejo Superior de Investigationes Científicas, CSIC-Universidad de Zaragoza, E-50009 Zaragoza, Spain.*
[d] *Departamento de Física de la Materia Condensada, Universidad de Zaragoza, Zaragoza, E-5009, Spain*

1 Constrained EPSR models of proposed Cu^{2+} hydration structures

The Empirical Potential Structure Refinement (EPSR) method is a particularly useful method for structural model building, as it allows us to test how our preconceived ideas can be accommodated by the information contained in the experimental data against which atomistic models are refined. For the case of the hydration structures of the Cu^{2+} aqua-ion, two prevailing models exist in the literature. The first model is the long-standing six-fold coordinated Jahn-Teller distorted octahedral hydration shell model, and the second is the more modern five-fold coordinated trigonal bipyramidal hydration shell structural model. By biasing the structure refinement process to favour each of these local environments in turn, it is possible to see whether they are consistent with the experimental data obtained from a real solution. For completeness three constrained structural models were investigated along-side the free refinement performed in the main scientific report and these constraints are illustrated in Figure 1.

1.1 Model 1: The square planar constraint model

In this structure refinement, the EPSR model was biased to favour the presence of four water molecules in a square planar geometry defining an equatorial plane about the Cu^{2+} ion. This model leaves the axial regions above and below the ion free for the EPSR procedure to populate with water molecules if the information in the experimental data requires their presence. In general, this model favours the generation of the traditional Jahn-Teller distorted octahedral hydration shell environment, but also allows for the presence of square pyramidal hydration shells, if only one of the axial positions is filled.

1.2 Model 2: The triangular planar constraint model

In this constrained refinement, the model was biased to favour the presence of three water molecules in a triangular planar geometry around the equatorial plane of the Cu^{2+} ion. Like the square planar model, this constraint leaves the axial regions free for population by the structure refinement process. This model
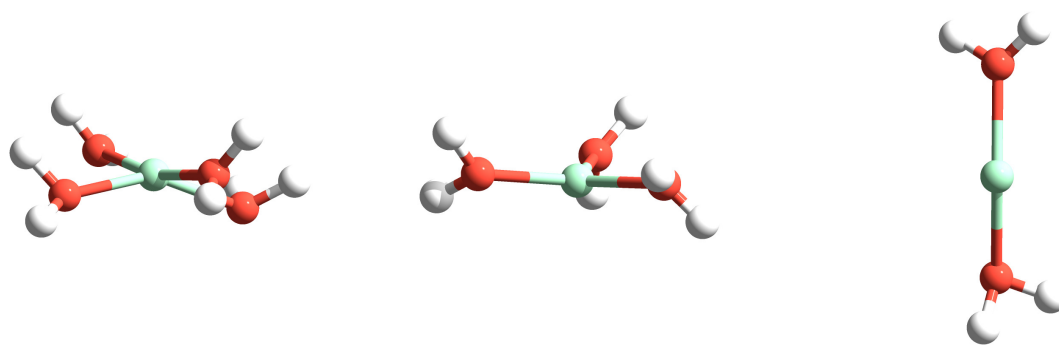
Figure 1: Illustration of constraint models used to test the sensitivity of the EPSR structure refinement procedure for modelling the neutron and X-ray scattering data on 0.5m and 2.0m $Cu(ClO_4)_2$ in water. The left hand structure illustrates the square planar constraint model where the structure refinement is biased to favour four water molecules in the equatorial plane of the Cu^{2+} ion leaving the axial positions free for population or not, via the structure refinement process. This favours the generation of locally octahedral hydration structures. The middle structure illustrates the triangular planar constraint model where the structure refinement favours three water molecules in the equatorial plane of the Cu^{2+} ion. This model favours the generation of trigonal bipyramidal hydration structures when the axial positions are filled. The right hand structure illustrates the axial constraint model, where two water molecules are constrained to occupy the axial positions favoured by the Jahn-Teller distorted octahedral environment or a trigonal bipyramidal hydration structure, and the structure refinement is then left to fill the equatorial region around the Cu^{2+} ions as best fits the data.

favours the generation of trigonal bipyramidal hydration shell structures and allows us to test the more modern proposal for the structure of the aqua-ion.

1.3   Model 3: The axial constraint model

This third model is biased to favour the presence of two axial water molecules, effectively leaving the equatorial region free for population by the structure refinement process. This allows the EPSR procedure to generate either octahedral or trigonal bipyramidal structures depending on the information contained in the experimental data.

2   Constrained model results

Figure 2, Figure 3 and Figure 4 show the results obtained from the three constrained structural models for the 0.5m and 2.0m solutions of $Cu(ClO_4)_2$ in water. In all three cases, the X-ray diffraction and EXAFS data highlight limitations in the ability of the models to closely reproduce all the available structural information. The best of the constrained models is the triangular planar constraint model that favours the more modern view of a five-fold coordinated hydration shell structure in a trigonal bipyramidal geometry, but this is still not as good as the free model, favouring the presence of significant numbers of tetrahedral sites, that is reported in the main text.
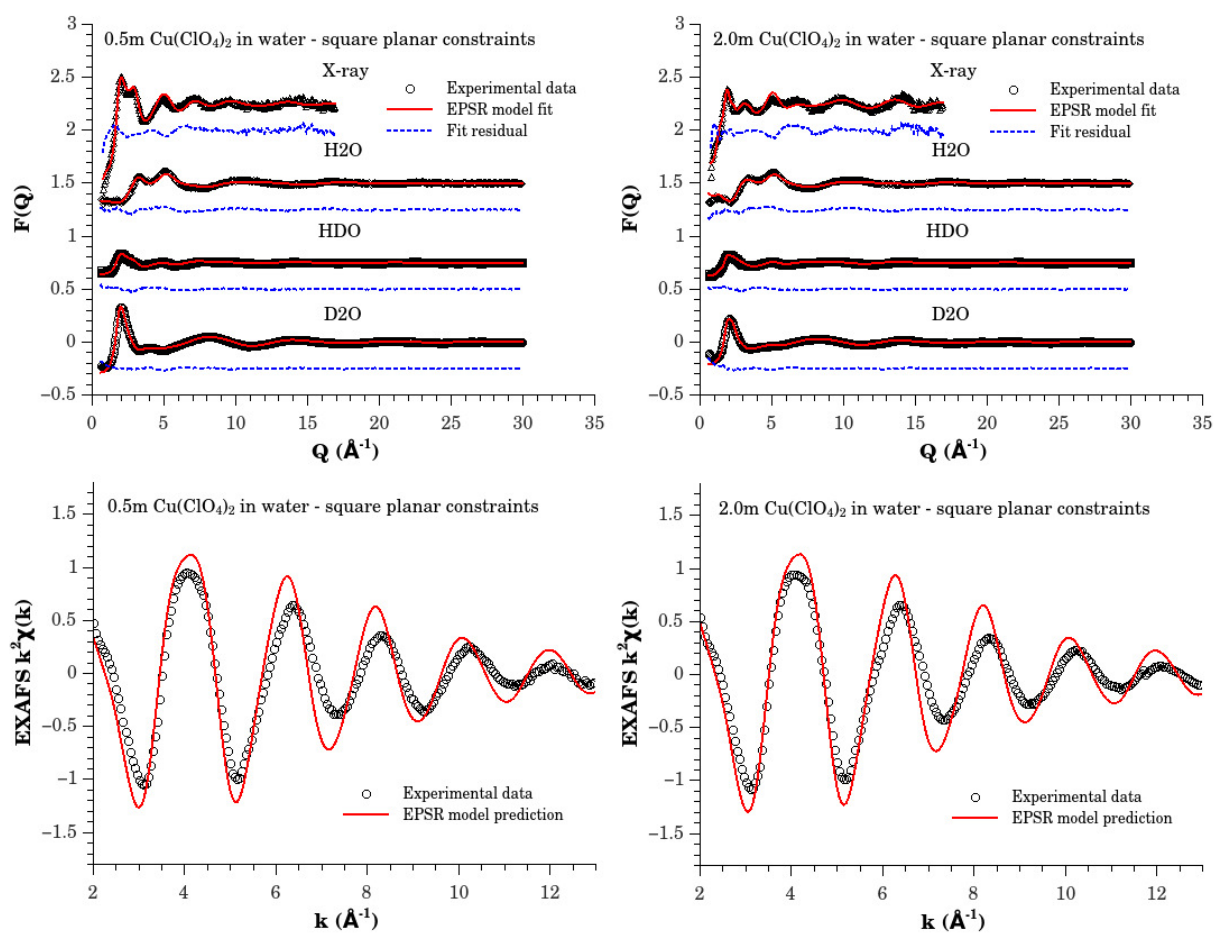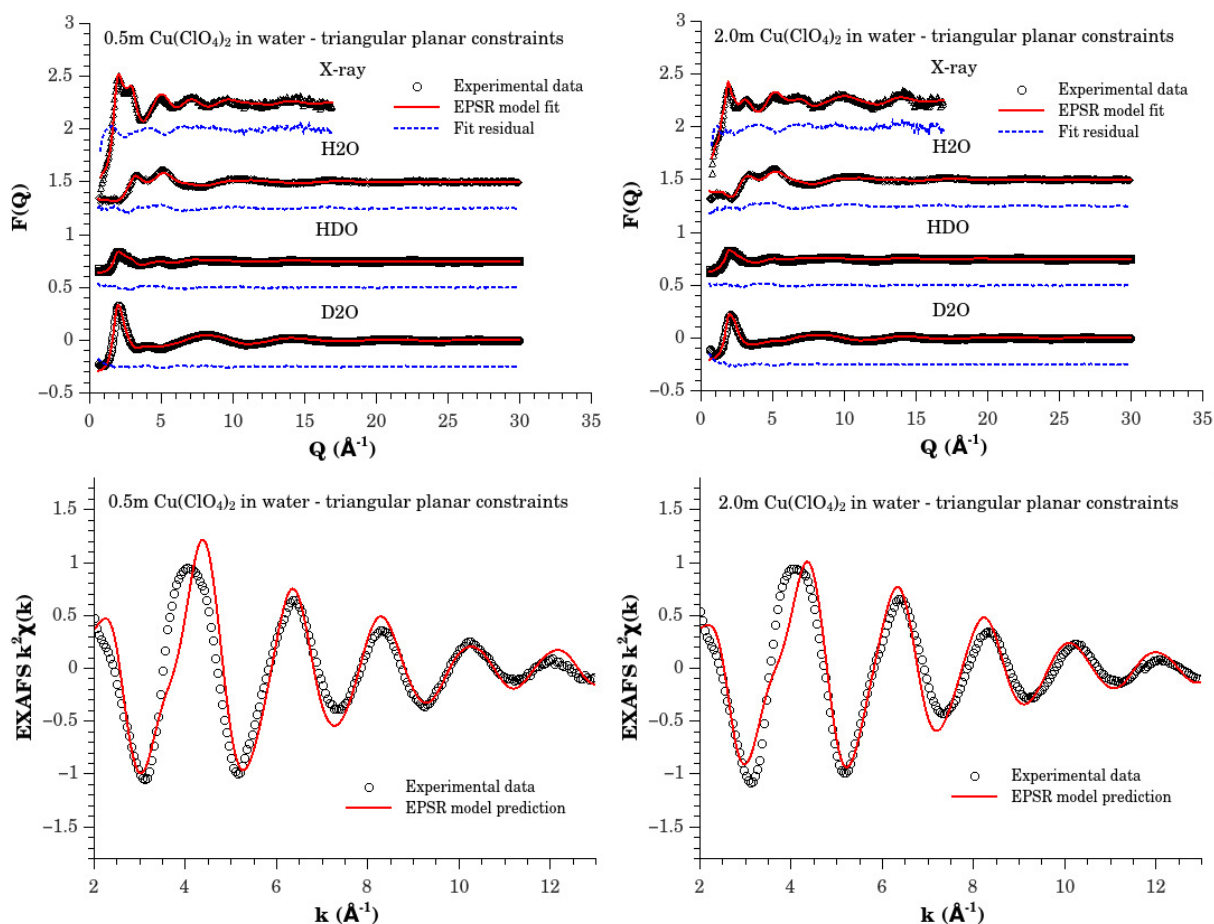
Figure 2: *Square planar constraint model:* The upper panels show the EPSR model fits (red solid line) and fit residuals (blue dotted line) to the isotopic samples of 0.5m (left panel) and 2.0m (right panel) $Cu(ClO_4)_2$ solutions prepared from D_2O, HDO, and H_2O measured by neutron scattering, and the $Cu(ClO_4)_2$ in H_2O solutions measured by X-ray scattering. The experimental data are shown as black circles. For clarity the model fits and experimental data are vertically offset by 0.0, 0.75, and 1.5 units, for the D_2O, HDO, and H_2O solutions respectively and 2.25 units for the X-ray data, while the corresponding fit residuals are vertically offset by -0.25, 0.5, 1.25 and 2.0 units. The lower panels show the resulting EPSR predication of the EXAFS signals arising from the applied bias towards octahedral local hydration shell geometries.

3

Figure 3: *Triangular planar constraint model:* The upper panels show the EPSR model fits (red solid line) and fit residuals (blue dotted line) to the isotopic samples of 0.5m (left panel) and 2.0m (right panel) $Cu(ClO_4)_2$ solutions prepared from D_2O, HDO, and H_2O measured by neutron scattering, and the $Cu(ClO_4)_2$ in H_2O solutions measured by X-ray scattering. The experimental data are shown as black circles. For clarity the model fits and experimental data are vertically offset by 0.0, 0.75, and 1.5 units, for the D_2O, HDO, and H_2O solutions respectively and 2.25 units for the X-ray data, while the corresponding fit residuals are vertically offset by -0.25, 0.5, 1.25 and 2.0 units. The lower panels show the resulting EPSR predication of the EXAFS signals arising from the applied bias towards trigonal bipyramidal local hydration shell geometries.
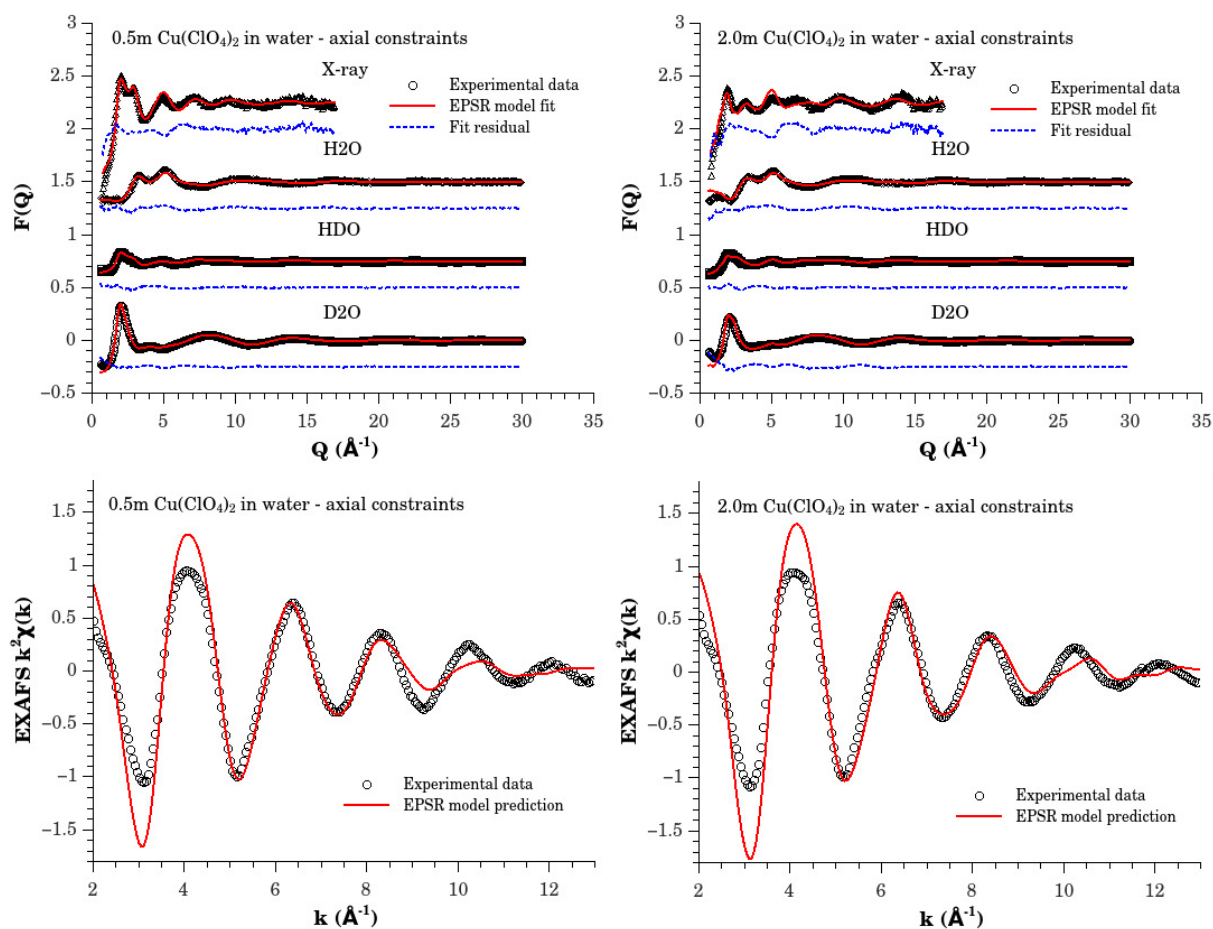
4

Figure 4: *Axial constraint model:* The upper panels show the EPSR model fits (red solid line) and fit residuals (blue dotted line) to the isotopic samples of 0.5m (left panel) and 2.0m (right panel) $Cu(ClO_4)_2$ solutions prepared from D_2O, HDO, and H_2O measured by neutron scattering, and the $Cu(ClO_4)_2$ in H_2O solutions measured by X-ray scattering. The experimental data are shown as black circles. For clarity the model fits and experimental data are vertically offset by 0.0, 0.75, and 1.5 units, for the D_2O, HDO, and H_2O solutions respectively and 2.25 units for the X-ray data, while the corresponding fit residuals are vertically offset by -0.25, 0.5, 1.25 and 2.0 units. The lower panels show the resulting EPSR predication of the EXAFS signals arising from the EPSR model that was free to generate both octahedral or trigonal bipyramidal local hydration shell geometries as required by the provided experimental data.

3   XANES pre-edge peak fitting

To estimate the intensity in the pre-peak at ≈ 8977eV in the X-ray absorption spectrum, the spectral region has been modelled with a series of Gaussian and Lorentzian peaks for the two solutions that have been investigated in the main paper (0.5m and 2.0m solutions of $Cu(ClO_4)_2$ in water), and also for two crystalline compounds ($Cu(ClO_4)_2.6H_2O$ and $CuSO_4.5H_2O$) in which copper in known to be coordinated by six oxygen atoms in an octahedral environment. Figure 5 shows the fits to the experimental data and Table 1 gives the refined peak parameters. For consistency all spectra were modelled using four functions: an error function to model the edge step, two Gaussian peaks to model the main absorption edge features and a Lorentzian peak to model the pre-peak of interest. All fits were performed using the *Athena* package (*ATHENA, ARTEMIS, HEPHAESTUS: Data analysis for X-ray absorption spectroscopy using IFEFFIT* B. Ravel and M. Newville, *J. Synchroron Rad.* **12** pp 537-541 (2005)).

Table 1: Peak fitting parameters used to model the XANES region of 0.5m $Cu(ClO_4)_2$ in water, 2.0m $Cu(ClO_4)_2$ in water, $Cu(ClO_4)_2.6H_2O$ and $CuSO_4.5H_2O$.

System	Function	Centroid eV	Amplitude Area	Width eV
0.5m $Cu(ClO_4)_2$	erf	8988.48	0.470	3.576
	Gauss	8996.03	4.007	2.626
	Gauss	9001.48	1.100	2.137
	Loren	8978.72	0.385±0.048	8.523±1.507
2.0m $Cu(ClO_4)_2$	erf	8988.48	0.473	3.644
	Gauss	8996.03	3.887	2.608
	Gauss	9001.48	1.154	2.169
	Loren	8978.72	0.378±0.055	8.732±1.806
$Cu(ClO_4)_2$	erf	8993.14	0.543	8.322
	Gauss	8995.12	7.498	3.872
	Gauss	8988.41	0.611	1.369
	Loren	8977.45	0.142±0.161	3.616±5.810
$CuSO_4$	erf	8993.14	0.578	8.490
	Gauss	8995.26	5.899	3.083
	Gauss	8989.37	1.272	1.328
	Loren	8977.25	0.114±0.224	3.018±8.417

This analysis procedure has highlighted the difficulty in obtaining reliable estimates of the pre-peak intensity when the feature of interest is extremely small $< 5\%$ of the normalised edge step. Although the trend seems to indicate increased intensity for the quadrupolar transition at ≈ 8977eV, this is strongly dependent upon the methodology adopted to model the main edge features that unavoidably vary between different samples. As a result, we feel it is unsafe to use this feature as strong evidence for components of local tetrahedrally in the solutions investigated.
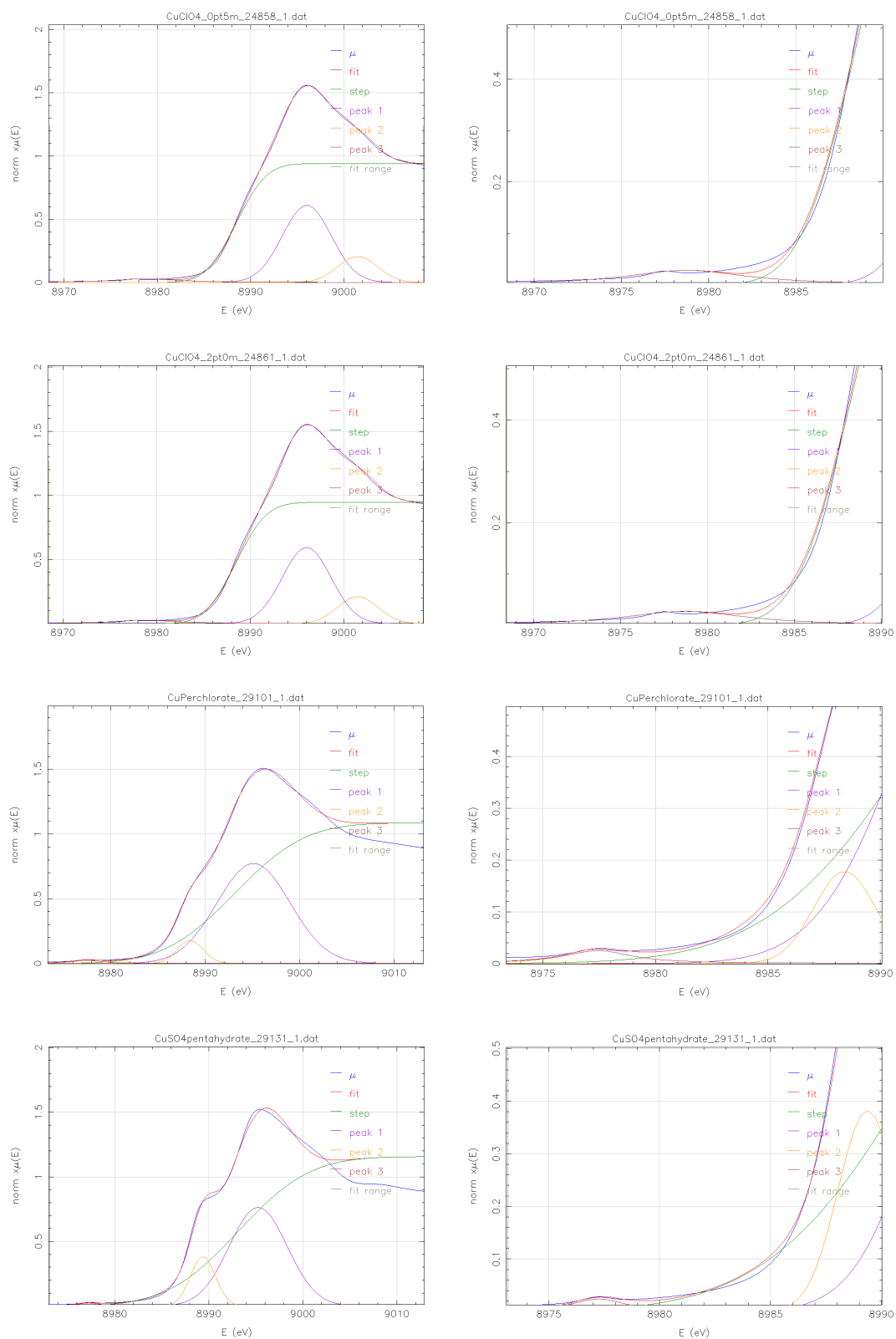
Figure 5: Multi-peak fit to the XANES region of the X-ray absorption spectra for (top to bottom) 0.5m $Cu(ClO_4)_2$ in water, 2.0m $Cu(ClO_4)_2$ in water, $Cu(ClO_4)_2.6H_2O$ and $CuSO_4.5H_2O$. For consistency, each dataset was fit in the energy region ± 20eV about the Cu K absorption edge using an error function to model the absorption step, two Gaussian peaks to model the main absorption edge, and a Lorentzian peak to model the dipole forbidden quadrupolar transition at ≈ 8977eV. The left hand panels show the fits over the full region of interest whilst the right hand panels are zoomed into the pre-peak range.